Funded by the
European Union

Transboundary Storm Risk and Impact Assessment in Alpine Regions

CROSS-BORDER RISK ACTIVITIES IN THE PILOT AREAS

Deliverable 4.5

REVISION n.: [01]	DATE: [30/06/2022]	
DISSEMINATION LEVEL: [Public]	WP: 4	TASK(s): 4.5
AUTHORS:	Massimiliano Pittore, Kathrin Renner, Piero Campalani, Alice Crespi, Sebastian Lehner, Katharina Enigl, Fabrizio Tagliavini, Matthias Plörer	

Project duration: January 1st 2021 – December 31st 2022 (24 Months)

Main changes compared to previous version	Page(s)

TABLE OF CONTENTS

1 INTRODUCTION

The purpose of this document is to describe the risk-related activities carried out in the three main cross-border pilot areas of the TRANS-ALP project. All activities have been designed as cross-border, also due to the neighbouring relationships of the involved countries and the scope of the project. Each pilot areas contributed to such cross-border activities according to the different skills, capacities and data / resource availability, and also carried out other complementary activities. Both these types of activities are described in the following, either in the first section, dealing with the common, overarching activities or in the second section where the location-specific activities are considered. Each activity is briefly discussed, with more details to be found in the corresponding project deliverables, to which references are given in the text.
In the conclusions section several further remarks are given.

2 CROSS-BORDER RISK ACTIVITIES

1.1.1 EXTREME EVENTS IMPACT MAPPING

In the Deliverable 2.2 [1] we laid the focus on the identification of extreme events affecting the cross-border region between Austria and Italy. Within this deliverable, gridded precipitation data for Austria and South Tyrol were collected and used for the purpose of event identification (see the individual sections later in the document).

Through a statistical analysis 12 events between 1980 and 2020 have been identified, whose dates of occurrence as well as the local maximum in South Tyrol (ST) and Austria (AT) are depicted in the following table:

Table 1 Events selected as significant according to the 99th percentile methodology.

Event date	Local max (AT)	Local max (ST)
18.07.1981	157,7	128,5
31.01.1986	166,6	162,9
25.11.1990	93,60	173,4
02.10.1993	151,0	144,3
20.09.1999	157,2	144,6
01.11.2003	158,7	127,3

29.10.2008	92,0	148,0
27.05.2011	91,5	150,6
05.11.2014	248,1	195,7
25.08.2018	72,7	119,7
29.10.2018	212,0	184,6
01.02.2019	103,2	240,5
15.11.2019	118,6	166,3
29.08.2020	115,30	107,4
05.12.2020	251,5	274,4

These events are deemed extreme in statistical sense, based only on precipitation data, and is associated with widespread impact and consequences in the three pilot areas.
Each event has been then considered individually, and all available meteorological data for the pilot areas for the related timeframe have been collected to provide a consistent representation of the event for further risk analysis. Furthermore, data on the degree of anomalousness of the event have been included. An example, related to the 2018 Vaia storm, is provided in the following. Further details are available in deliverable D2.3 [2].

28.10. - 30.10.2018 (Vaia/Adrian)

In the evening of 26.10.2018, a trough of low pressure strengthened over the western Mediterranean Sea, which led air masses from the Mediterranean Sea to the northeast and could strengthen into a vortex – called VAIA - in the further course.
Although the vortex was still weak on October 27th, many places already received heavy rainfall on this day. Especially in northern Italy, southeastern Switzerland and southwestern Austria, there were several severe weather warnings. The snow line was between 1500 and 2000 m in the Southern Alps. Repeatedly, interspersed showers and partly also thunderstorm cells formed, which even in the lowlands, such as in Vaduz, included one-hour rain shower values of up to 28 mm by 8 p.m. CET. In addition, a strong temperature drop occurred, which allowed snowfall down to lower elevations. The largest 24-hour precipitation value by 07:00 CET the following day occurred in the Lepontine Alps in southern Switzerland with 136 mm of precipitation in Robièi. In Carinthia, precipitation was similarly high with as much as 138 mm in Dellach im Drautal. Overall, there was heavy precipitation across the area from Italy to southern Germany. The next day, Oct. 28, the

vortex VAIA continued to lie over the western Mediterranean Sea only about 100 km to the south. The counterclockwise rotation allowed large amounts of evaporative moisture to be absorbed over the warm Mediterranean Sea. In addition, a blocking situation was present since an area of high pressure was located over North Africa. However, this allowed low VAIA to absorb moisture and heat over a longer period of time. On this day, the weather character of the previous day remained similar, with precipitation levels increasing once again. On this day, similar regions were again affected by advective precipitation over long periods, so that there was also a threat of flooding. In Kötschach, 105 mm of precipitation again fell in the 24-hour interval until 07:00 CET, so that about 180 mm had fallen in the past 36 hours. Also the Drau valley was still represented with 79 mm at the peak values, here should still follow a flood HQ30 to HQ100, i.e. with statistically calculated 30- to 100-year recurrence. Problematic in Carinthia and northern Italy was the rising snow line on 28.10., which was partly well above 2000 m. The surface runoff was therefore very high up to the valley. As a result, surface runoff reached the high mountains and the flood situation came to a head. Several mudslides were also reported, forcing the closure of the Brenner freeway, among others. On 28.10. the wind gusts on the front side, i.e. in Austria and Italy, also reached storm character. The highest measured gust was 157 km/h on the Rossalm in South Tyrol at 2300 m altitude. On the next day, similar conditions were observed in Austria, with the highest runoff expected in the evening. In Obergurgl at 2000 m in the Ötztal valley, 96 mm of precipitation fell, near the summit accordingly significantly more and especially in solid form. Thus, more than 2 m of fresh snow could be measured on the glaciers at 3000 m. The highest precipitation rate within one hour was recorded with a value of 85 mm at 3300 m on Piz Corvatsch.

Vaia brought severe conditions to Northern Italy and surrounding regions, causing over €3.3 billion in damages. Throughout Italy, 11 fatalities were reported. The storm damaged the Basilica of San Marco and left 75% of Venice underwater, but it also caused devastating damage to the Alpine forests south of the Dolomites.

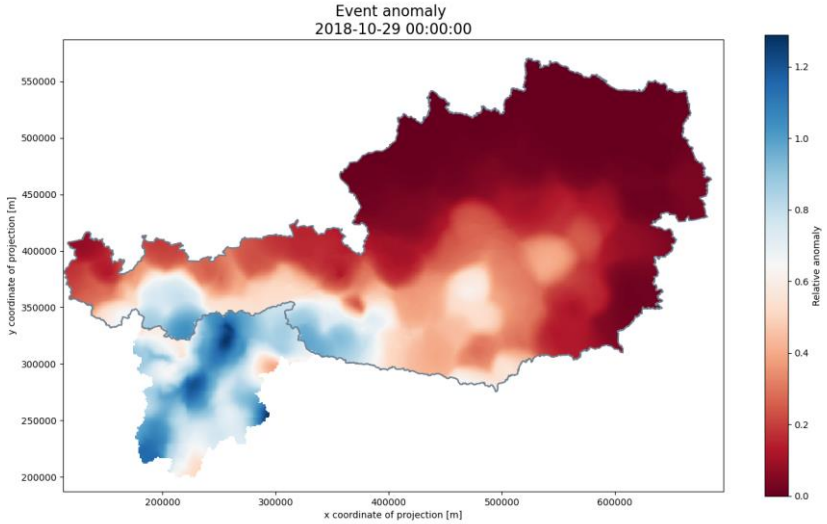

Figure 1 Relative anomaly of October 29th, 2018 based on the gridded datasets from Austria and Trentino-South Tyrol.

1.1.2 IMPACT ANALYSIS

In order to further explore the relationship between extreme weather and observed effects on the ground, a thorough collection of impacts has been carried out in Austria and Italy and the data analysed (see deliverable D2.3 [2]). Combining the data sets of the WLV and GBA for Austria with those of the IFFI and the ED30 database for South Tyrol and subsequently applying the translation scheme of the established vocabulary resulted in a so-called event space used for further analyses. The event space covers the period from 1961 to 2021 and stretches over Carinthia and East Tyrol in Austria as well as South Tyrol (Alto Adige) in Italy.

This newly established database includes 1302 events on the Austrian side; 672 of them describe flood events, 633 entries relate to mass movements – flows and slides. In the case of South Tyrol, the event space comprises 623 flood events and 2229 mass movements.

Figure 2 illustrates the spatial distribution of events, differentiated between hazard categories. The spatial density of flood events is highest in East Tyrol and in the border region to South Tyrol. The detailed figure for the recorded mass movements reveals the richness of the IFFI database for South Tyrol, covering nearly the entire South Tyrolean territory. The spatial coverage of events in Carinthia is considerably lower for both hazard types. A large number of flood events occur along the largest rivers in Carinthia; other flood events refer to small Alpine torrents.

The seasonal distribution of events for both hazard categories as well as target regions is demonstrated in Figure 3. When considering flood events, the pronounced maximum of registered events in the Austrian target regions occurs within the summer months (June, July, August). The right panel, however, indicates different results for South Tyrol; the maximum number of registered events appears in autumn (September, October, November). Considering mass movements, a similar picture emerges for South Tyrol and Carinthia/East Tyrol. The maximum of registered events occurs during summer, followed by the autumn months. Moreover, this figure also exhibits the number of registered mass movements in the Italian target region being significantly higher than those on the Austrian side.

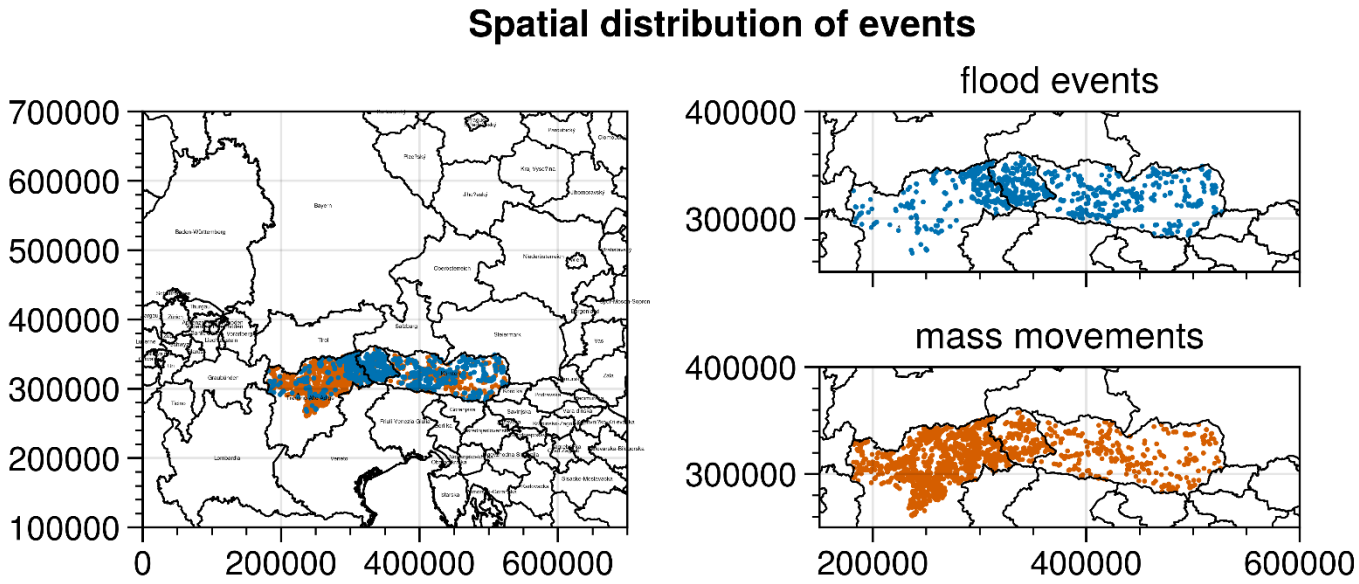

Figure 2 Spatial distribution of flood events (blue) and mass movements (orange) in the target regions Carinthia/East Tyrol and South Tyrol.

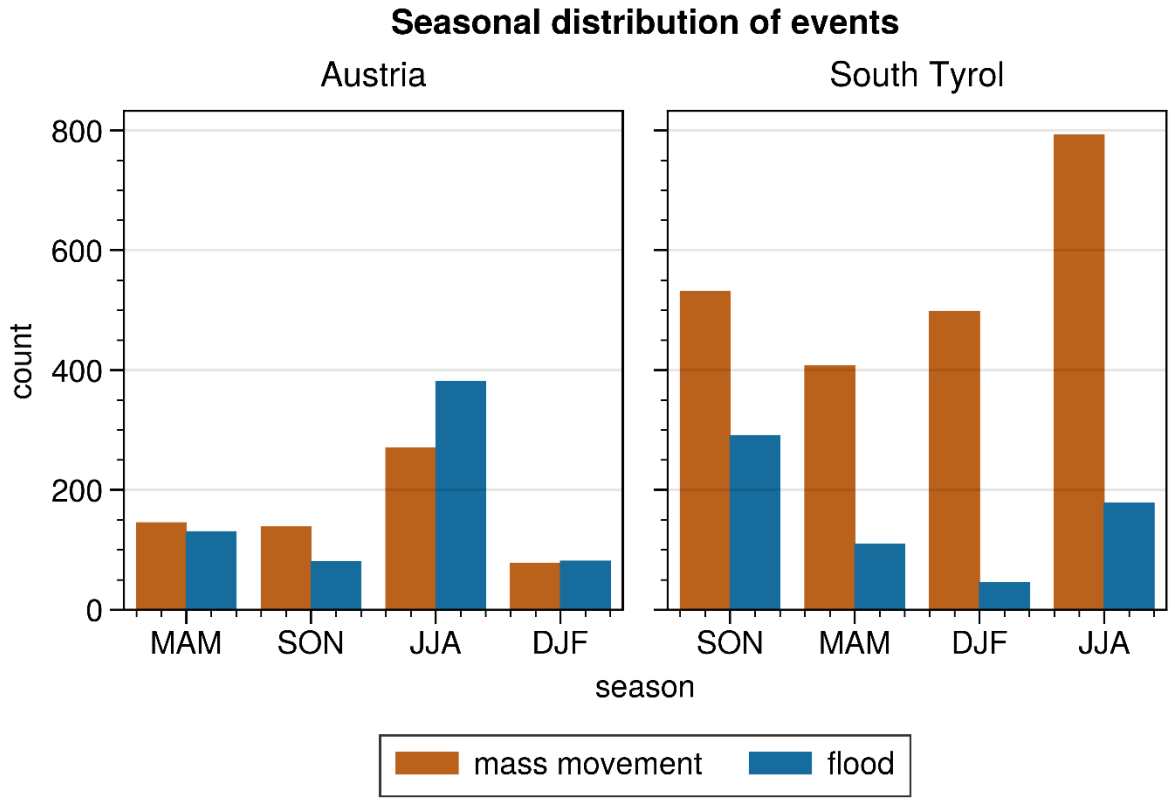

Figure 3 Seasonal distribution of flood events (blue) and mass movements (orange), differentiated between the two target regions Carinthia/East Tyrol and South Tyrol.

For different types of primary impacts (floods and mass-movements) a statistical analysis has been carried out to understand if specific temporal precipitation patterns can be associated to possibly damaging events. A selection of the obtained results is reported in the following pages. For further detail see Deliverable D2.3 [2].

2.1.1.1 Results for floods during autumn (SON)

Figure 4 and Figure 5 represent the results for the category “floods” in both target regions. Looking at the histogram of 8-day precipitation sums, it is revealed that the majority of events feature precipitation totals between 50 and 100 mm. This assessment for South Tyrol, however, illustrates strikingly different outcomes as most events exhibit precipitation sums of lower than 20 mm.

EOF1 in Figure 4 exhibits an explained variance of 28%. The weather sequence is characterized by high pre-moistening in the first half of the week which ends in a precipitation minimum on day 4 pre-event. After that, precipitation amounts rise and reach their maximum on the target day, with roughly the same weight as the peak of the pre-moistening. EOF2, featuring a simulated variance of 23%, also represents pronounced pre-moistening, especially from day 4 to 1 before the event, again indicating short-range pre-moistening. On the event day itself, precipitation recedes. EOF3, however, exhibits a weather pattern that is shaped by ups and downs, signifying variable precipitation the preceding week, without a strong consecutive signal either way.

Outcomes for South Tyrol depict different trigger patterns. EOF1, featuring a simulated variance of 34%, reveals a curve starting from high values on day 7 and continuously falling, with a temporary maximum on day two, until the event day. EOF 2 (explained variance of 21%) shows little precipitation amounts at the beginning of the precedent week, which steeply increase up to day 4 before falling again and reaching a minimum on day 2. The curve rises again up to the event day, giving the most importance to t-4 as well as immediate precipitation amounts. EOF3, having an explained variance of 16%, the pattern indicates pre-moistening in the medium-range, with a pause in between and increasing precipitation amounts up to the event day.

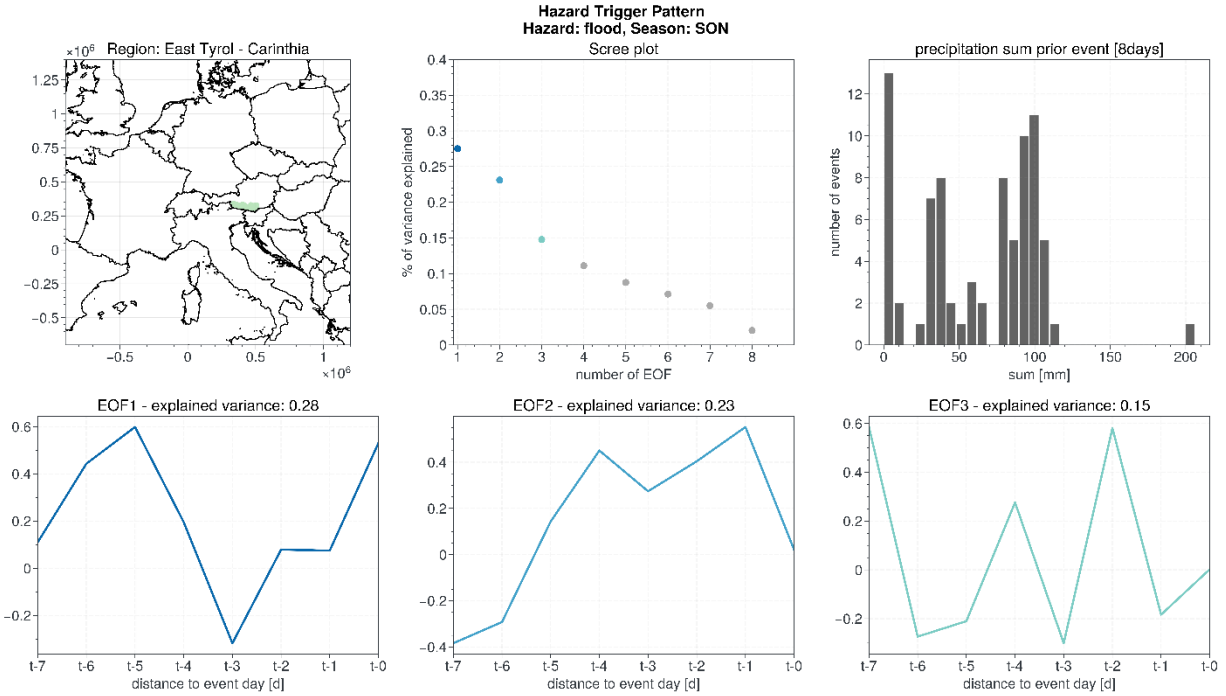

Figure 4 Hazard Trigger Patterns for floods in the target region Carinthia and East Tyrol for SON.

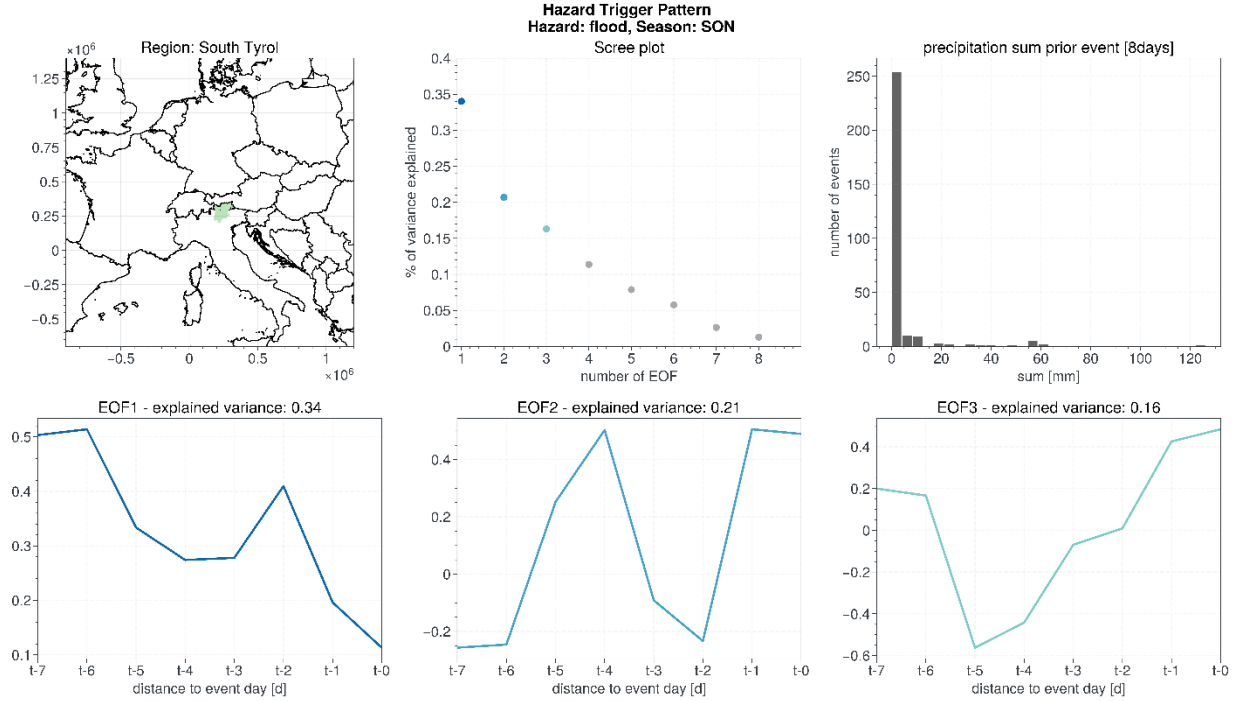

Figure 5 Hazard Trigger Patterns for floods in the target region South Tyrol for SON.

2.1.1.2 Results for mass movements during autumn (SON)

Figure 6 and Figure 7 refer to the outcomes for the hazard category “mass movements” during the autumn months September, October and November. Results for the Austrian target region “East Tyrol and Carinthia” indicate that the majority of events feature an 8-day precipitation sum before the event of 50 to 100 mm. EOF1, having a simulated variance of 28%, reveals pronounced premoistening conditions up to the short-range, illustrating high precipitation amounts from day 6 to day 1 prior the event. On the target day, however, precipitation decreases sharply with minimum importance. EOF2, featuring an explained variance of 16%, is characterized by “ups and downs”. The week before event occurrence starts with wet conditions before precipitation reaches its minimum on day 5. Subsequently, the curve rises steeply and arrives its maximum on day 2 before falling again. At the event day, precipitation amounts slightly increase again. EOF3, on the other side, indicates less precipitation in the first half of the precedent week and rising amounts from day 3 to day 1 pre-event occurrence. On the event day itself, however, the curve is decreasing.

Results for mass movement in the season SON for the target region South Tyrol show that the majority of events feature an 8-day precipitation sum between 0 and 50 mm. The first orthogonal function, showing an explained variance of 27%, reveals a similar pattern than EOF1 in the Austrian target region. It is characterized by pre-moistening, especially in the first half of the precedent week of event occurrence. In the second half, precipitation amounts lower significantly. EOF2 (explained variance of 25%) bears strong resemblance to EOF1 with a slight difference on the target day. In this pattern, precipitation rises again after having reached its minimum on day 2 and 1 prior the event. EOF3, featuring an explained variance of 14%, is also strongly influenced by pre-moistening, starting on day 7 before the event and reaching the maximum precipitation on day 3, before slightly decreasing again (see Deliverable D2.3 [2]).

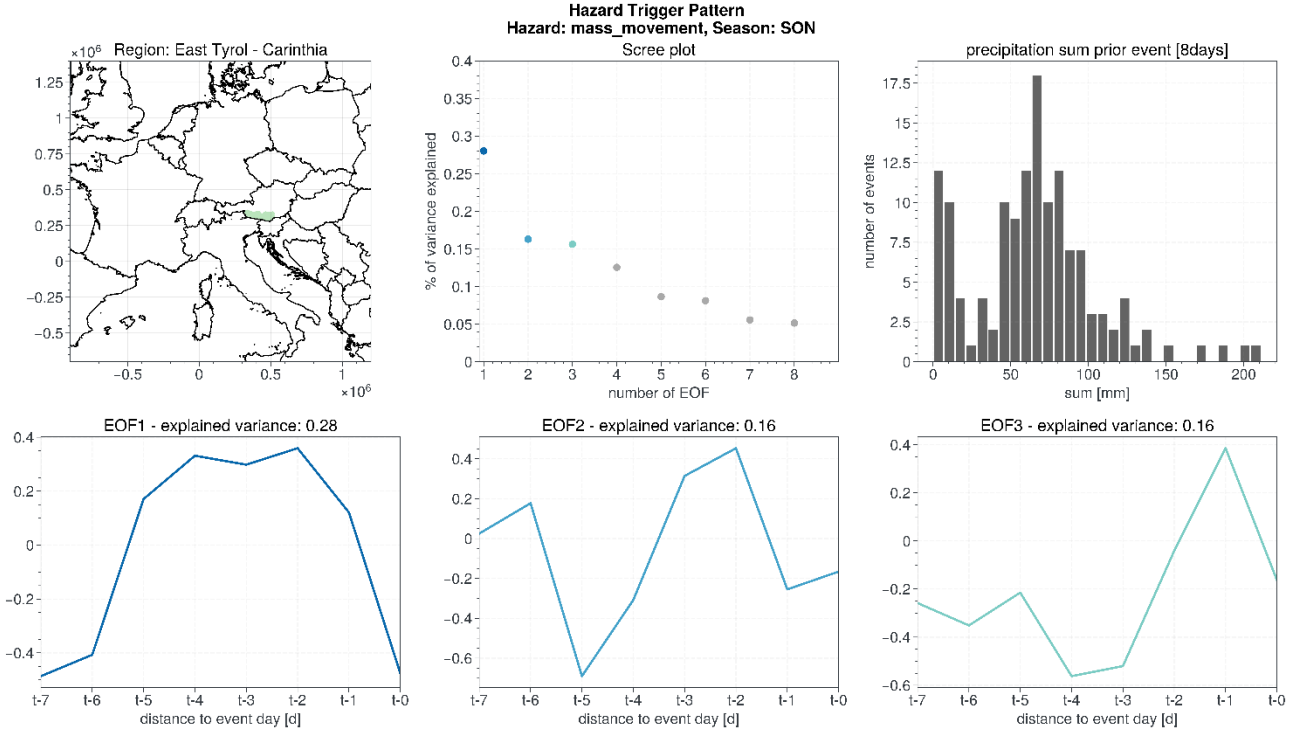

Figure 6 Hazard Trigger Patterns for slides in the target region Carinthia and East Tyrol for SON.

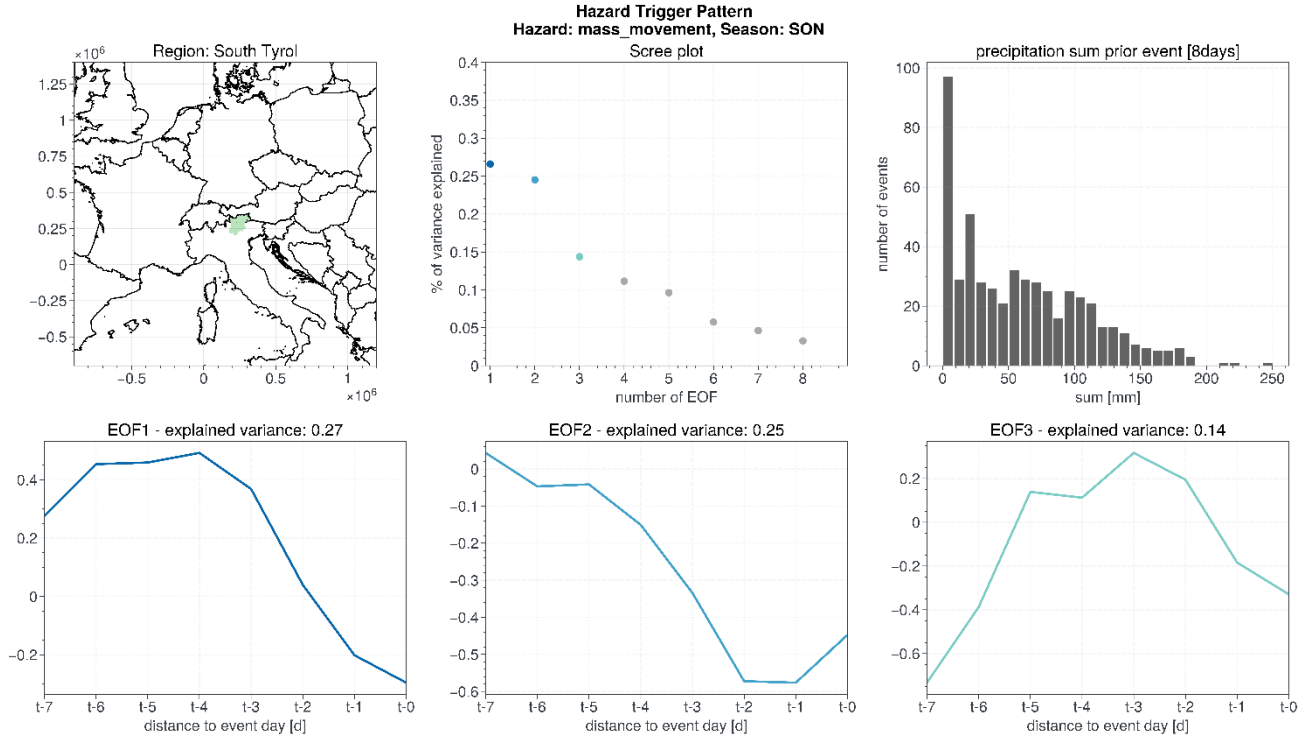

Figure 7 Hazard Trigger Patterns for slides in the target region South Tyrol for SON

1.1.3 Expected change in storm hazard in the future due to Climate Change

A further cross-border activity, **described in detail in the deliverable D2.4 [3]**, has explored the potential influence of climate change on the evolution of storm hazards in the future. In general, there are two focal points for future hazard development: Frequency and intensity. Both aspects share equal importance for risk reduction, as e.g., in the case of flooding. Successive hazard-events of medium intensity (i.e. higher frequency) can be just as devastating as one hazard-event with higher intensity. Furthermore, there are more faceted aspects to be considered, as higher intensity can simply be exhibited as higher values per fixed spatial extent, larger affected areas, or both.

The use of Hazard Trigger Patterns (HTPs; **for details refer to D2.1 [4]**) for the evaluation of potential hazard development is a two-step process:

The first step consists of defining the current climate state. Therefore, so-called “potential events” need to be determined in the past period. Potential events are events, that potentially could have caused damages due to the precedent weather evolution, but eventually did not.
HTPs originate from an PCA analysis of a two-dimensional matrix containing precipitation evolutions prior event occurrences (n rows for n events and precipitation values over 8 days in the precedent week) and represent the eigenvectors of this matrix. The corresponding “time coefficients” are referred to as “principal components (PCs)”. Methodologically, potential events can be identified by projecting meteorological data into the EOF space, generating so-called Pseudo Principal Components (PPCs). Subsequently, we compare the PPCs to the PCs from the observational data. A potential event is registered if the corresponding PPCs are within a certain Euclidean distance to the PCs. We determine the value of this distance by conducting a leave-one-out cross-validation procedure to evaluate the average distance between the PCs of the observations. This is done by iterating over all observations and computing the EOF analysis for all but one observation in each iteration. PPCs are then calculated for the omitted observation and the Euclidean distance to all PCs is computed. In each iteration step, we store the minimum of these distances. Finally, all iterations are averaged, and the resulting value represents the threshold below which PPCs are counted as a potential event.
The second step comprises the application of the same procedure as in step one to climate projections and the computation of hazard development corridors (HDCs). For a timeseries of the corresponding predictors of a grid point (or analogous to the HTP calculation: mean value over the respective grid point and the four adjacent grid points), a matrix is created that contains each possible 8-day sequence of this timeseries. This guarantees that all possible potential events can actually be found. This matrix is then transformed into the EOF space, generating PPCs for each of these 8-day sequences. By using the threshold value identified in step one, we can then determine for each of these sequences whether these represent a potential event. 20 random grid points per region are used to calculate the projections, which are shown in Figure 5.
The HDCs map the change in hazard potential by calculating potential events for both historical and future periods. The potential events for future periods are then normalized using the mean and standard deviation of the potential events derived in the historical period, thereby creating the so-called, hazard risk index. This index indicates the change in the hazard potential and thus represents a quantity that can be used for risk assessment. The content of this index, however, refers purely to the frequency of the underlying phenomenon and does not describe its amplitude which may be qualitatively estimated by means of the climate indicators for the corresponding damage categories.

Some climate indicators are also calculated as area-averages over the region of interest, in order to assess the potential development of intensity for hazardous damage event. Thereby, RR20mm, Rx5day and Rx1day are used. RR20mm depicts the number of days per year in which daily precipitation totals surpassed 20 mm. Rx5day is the annualized maximal precipitation sum for 5 consecutive days and Rx1day is similarly the annualized maximal precipitation sum for 1 day. Those indicators are calculated for the historical period as well as the future period.

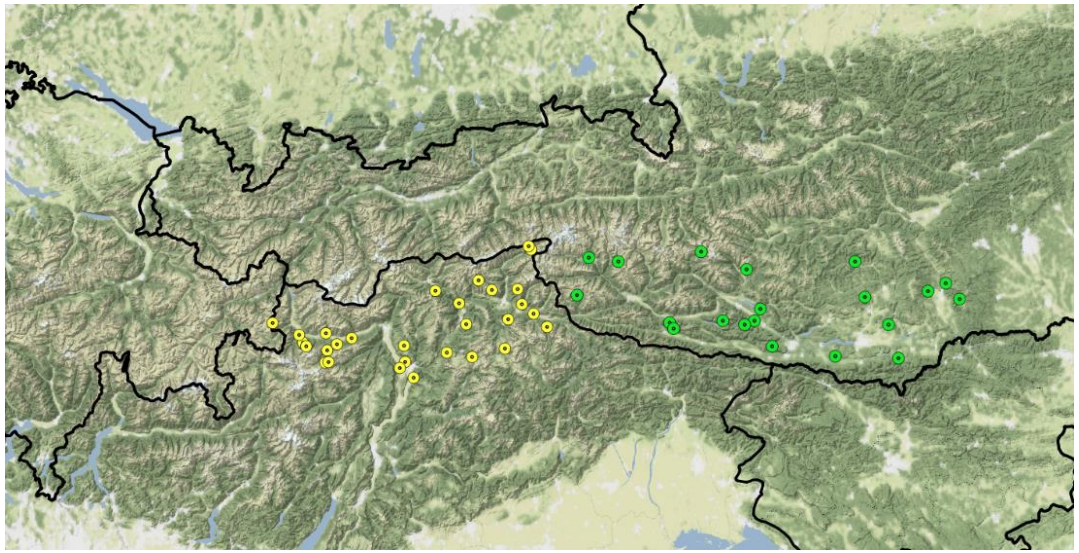

Figure 8 The 20 randomized grid points per region that were selected for the calculation of projections for hazard development corridors. Yellow coloured markers reside in the region ST, green coloured in ET_C.

An example of the obtained results is shown in the following, focusing only on the high percentiles of the considered models. Those situations depict the most extreme cases, that potentially cause the most losses. In Figure 9 the 90th percentile of the hazard risk index for models is shown as multi-model boxplot. The dashed black horizontal line serves again as reference to a standard normal distribution, wherein the 90th percentile is at roughly 1.28. A higher/lower multi-model median hence suggests an intensifying/relaxation of high impact risk potential respectively. There does not seem to be overwhelming support for a significant increase in the hazard risk index. Although, it has to be noted that the large variabilities, especially for the far future compared to the near future have to be carefully considered. This depicts some chance of a worsening development in terms of hazard event frequencies, with a larger number of potential events. Looking at the numbers for the summer season and far future (bottom row, second subplot from the left-hand-side) the multi-model median for the 90th percentile corresponds to roughly a value of the 97th percentile for a standard normal distribution. This is a substantial increase depicting a threefold increase in potential events at that rarity level. The other changes are not as pronounced and especially do not show such a substantial increase for the hazard risk index. Hence this situation should be investigated more carefully, taking into account more information from other sources.

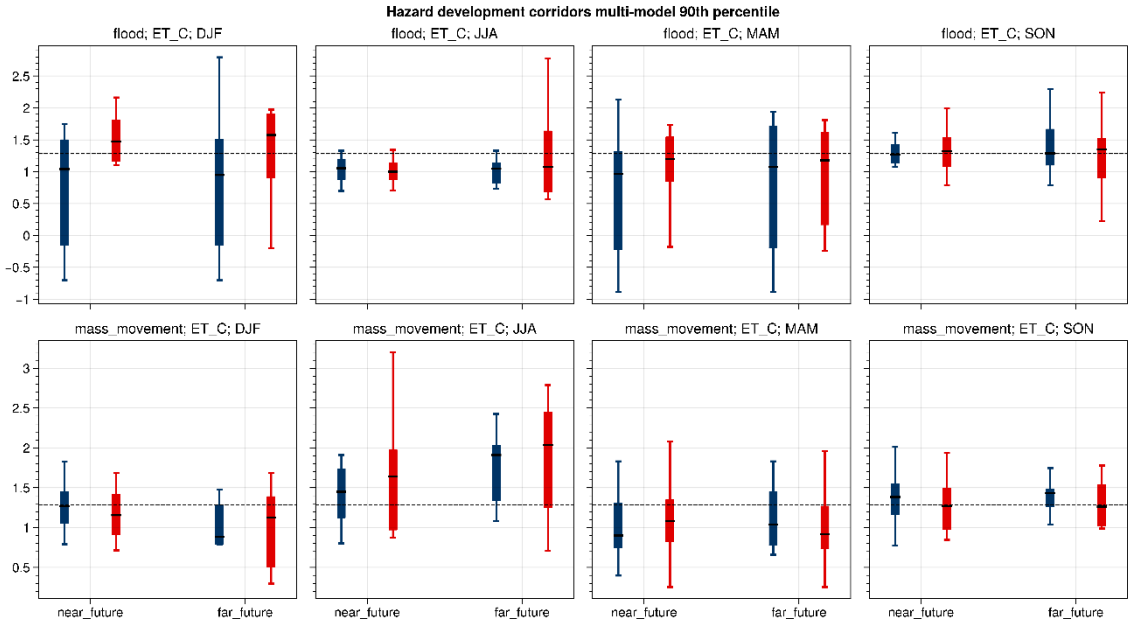

Figure 9 90th percentile of the normalized risk index is shown. The dashed black line represents the 90th percentile for a standard normal distribution and serves as reference point.

The results of the hazard development corridors show mixed signals with a substantial amount of superimposed noise. This is largely due to natural variability and some uncertainty originating from the methodology, due to the localized-nature of the technique.
All results combined, hazard development corridors, the annual potential increase in precipitation and the large fluctuations in high-impact climate indicators, it is evident that potential future risk increases have to be taken into consideration for high-impact assessments. The most damage is not done by the averages of the distributions, but by extremes and superimposed extreme states that are further escalated by a tendency of increasing risk potential in certain situations outlined above, which may have devastating consequences if not taken into consideration. **See deliverable D2.4 [3] for further details**.

1.1.4 EXPOSURE MODELLING

An integrated multi-hazard exposure model has been implemented over the whole cross-border pilot areas. This information includes several relevant exposed assets related to the socio-economic system: building structures, people (including children and elderly), tourists, hospital and day-care system, as well as road transportation. In the case of forested areas, this parameter conveys both exposure and environmental

information, and is associated to land-use/land-cover information. These parameters provide an efficient and integrated support for risk assessment in case of storms and other complex events including multiple natural hazards. The model can be extended to encompass further information to improve the thematic resolution of the exposure model and to accommodate for further hazards of interests (see deliverable D4.3 and D4.4 [5], [6] for further details).

Table 2 Basic cell summary and cell-based statistics of the countable exposed assets considering the South-Tyrol area.

component	Count	Mean	std	min	max
No. of residents	13089	40.0	108.9	1	1715
Capacity tourism accommodations	4534	41.9	65.7	1	811
Capacity schools	494	173.3	277.2	5	2497
Capacity Elderly care centres	75	59.2	31.5	21	170
Beds day-care hospitals	7	24.3	24.9	4	78
No. Hospitals	7	1.0	0	1	1
No. Elderly care centres	75	1.0	0.1	1	2
No. of Tourists accommodations	4911	2.0	2.4	1	31
No. of schools	499	1.7	1.0	1	-

In Table 2 a basic cell summary and cell-based statistics of the countable features of the exposure model considering South-Tyrol (only where the corresponding cell attribute is greater than zero) is provided. We can for instance note that over 13’000 cells have a non-zero number of residents, with a maximum number of residents per cell equal to 1’715.

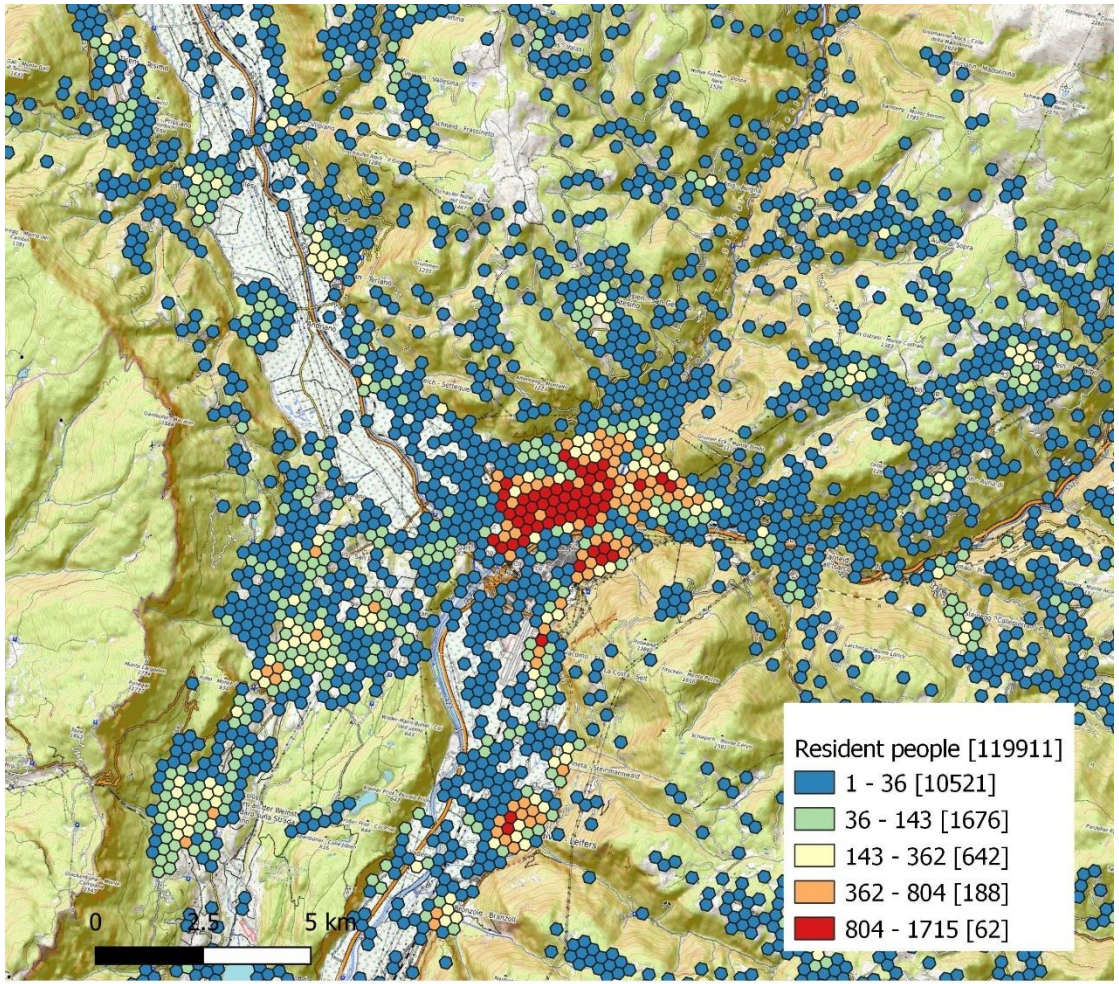

Figure 10 — Integrated exposure model: distribution of resident population (aggregated total number of people, only non-zero cells visualized). In parenthesis the number of cells related to the different value ranges.

Two visualizations of the resulting exposure model are provided in Figure 10 and Figure 11, respectively showing the distribution of resident population and the distribution of aggregated school capacity in the area of Bolzano, in South Tyrol. Only non-zero cells are displayed. We can

note that, being the information on the different exposed assets already aggregated at the cell level, it is straightforward to visualize (or use in further processing steps) the related features.
This harmonization allows for an easier employment of the resulting model in risk-oriented applications.
We can also note that the exposure information provided in the model is strictly related to the expected vulnerability of the assets with respect to the considered natural hazards, even in the case where vulnerability or sensitivity factors were not explicitly considered. For instance, the number and total capacity of schools provides information on the potential presence of children in the area, whereas the number and total capacity of elderly care centres is a proxy for the presence of elderly people.

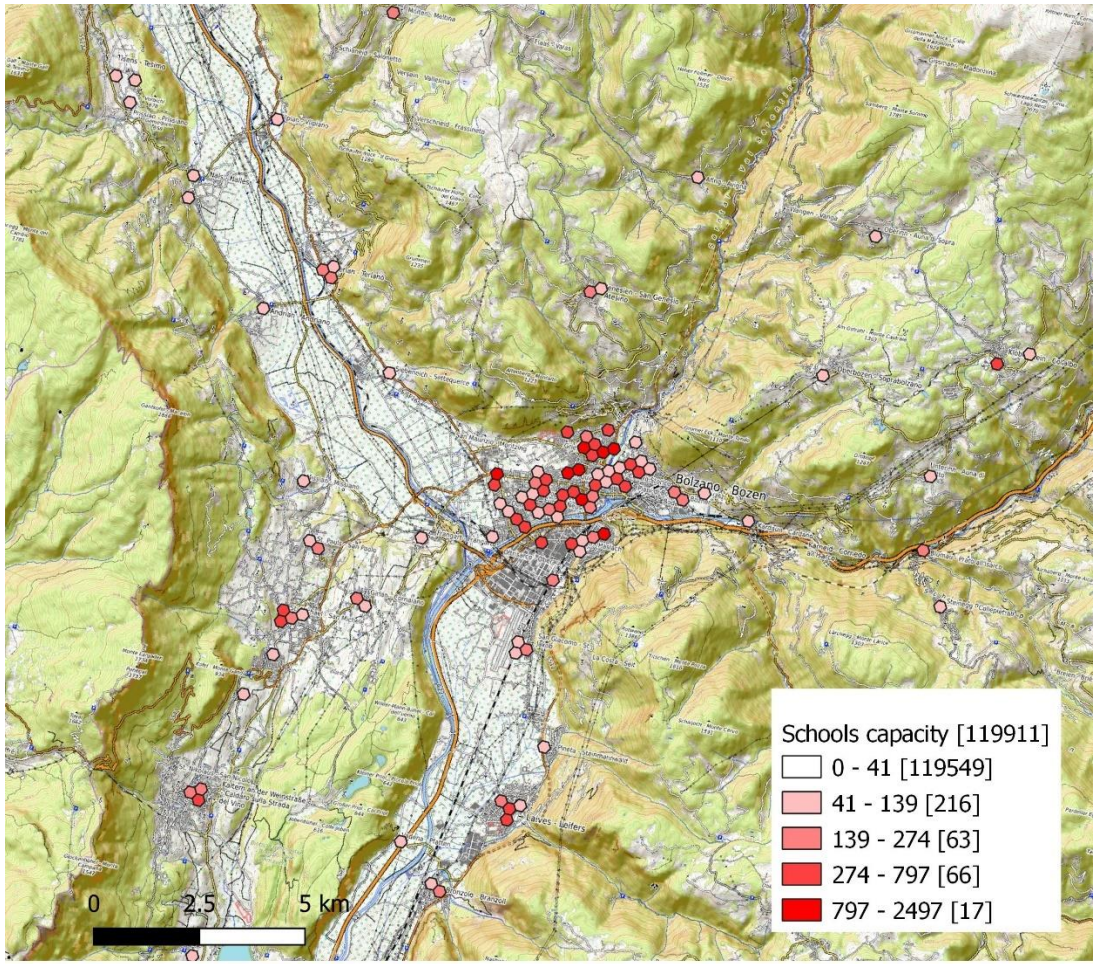

Figure 11 — Integrated exposure model: distributio of school capacity (aggregated number of pupils, only non-zero cells visualized). In parethesis the number of cells related to the different value ranges.

The aggregated description of the static assets has been integrated by a joint functional model of the transportation network, based on the same hexagonal tessellation. This model is obtained through a topological simplification procedure which accounts for the actual road network

by projecting it over the cell-based model. A cutout of the resulting simplified model (represented by a graph) over the municipality of Bozen/Bolzano is shown in Figure 12 (see Deliverable D4.3 [5] for further details).

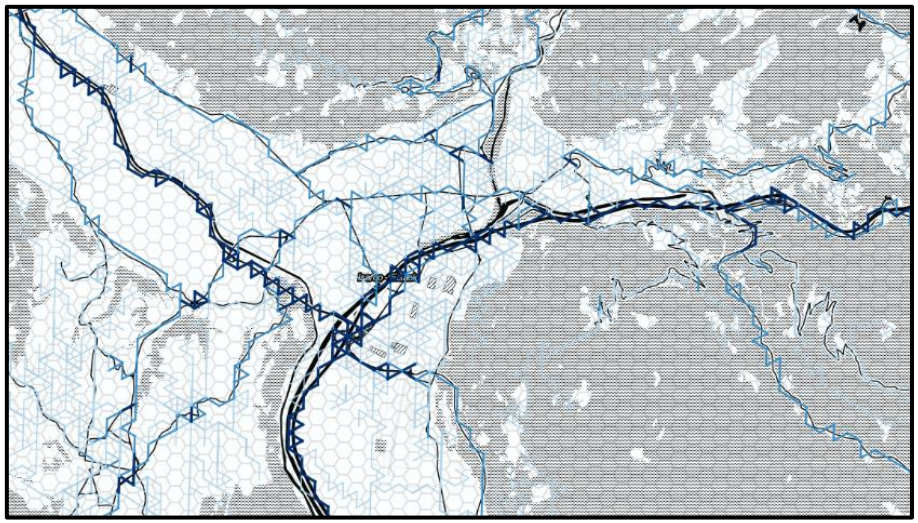

Figure 12 — Visualization of the drivable OpenStreetMap (OSM) roads graph over the area of Bozen/Bolzano after being projected onto the hexagonal tessellation. The original OSM roads dataset are also visible in the map. The gradient of blues and thickness of the edges in the graph encode the weight assigned to each edge in the simplified graph.

In Figure 13, the equivalent graph and the underlying aggregation boundary (i.e., the hexagonal tessellation) are shown. The resulting structure is providing a consistent modelling of both the exposed assets (aggregated over the cells of the tessellation) and the topological connectivity among the cells of the tessellation induced by the underlying road network. The hexagonal shape of the cell allows for a smoother representation of the connectivity while the weighting scheme used to aggregate the raw information on the roads provide a good indication of the total road capacity in each cell.

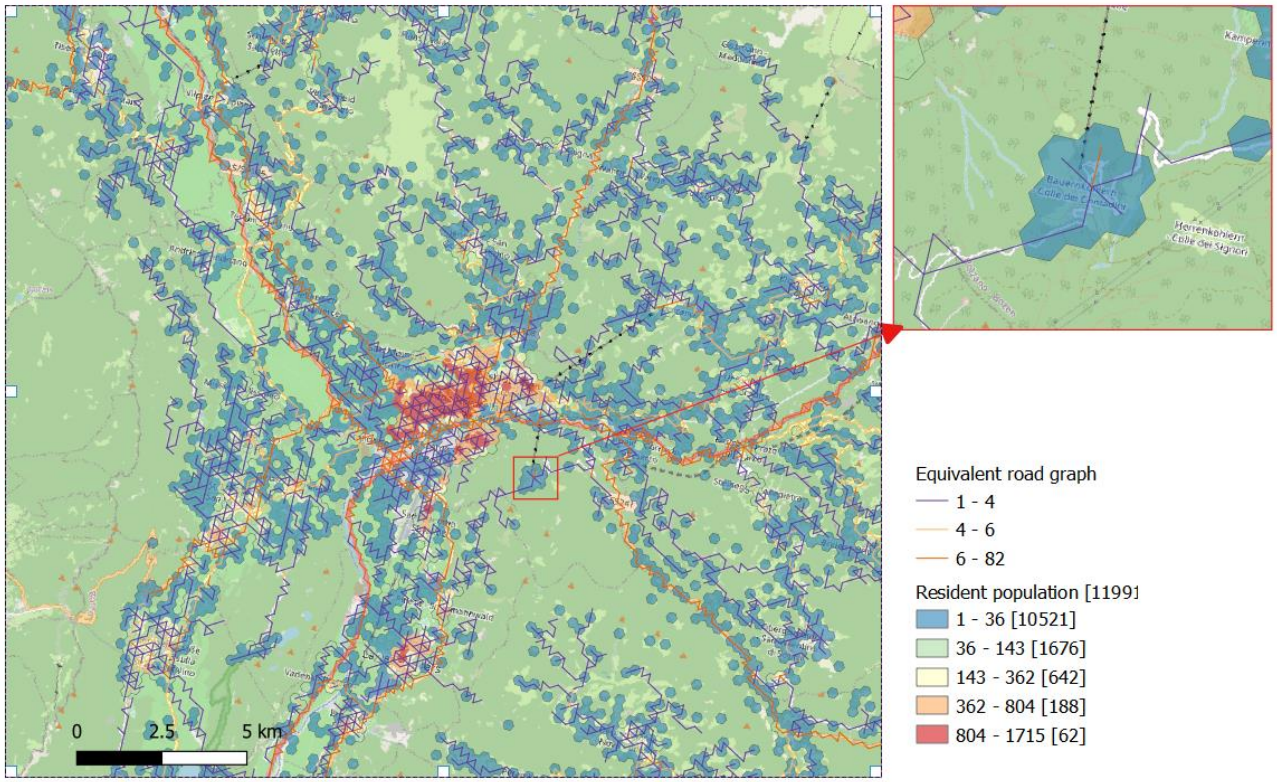

Figure 13 — Visualization of the integrated exposure model including the aggregation boundary (hexagonal tessellation) and the equivalent graph model, color-coded according to the intensity of connectivity.

The resulting equivalent graph has 11’589 intersections, 55% of the non-simplified one, therefore indicating a strong reduction in the complexity of the functional and topological representation. Since the simplified connection takes into account the number and type of roads connecting neighbouring cells, this equivalent representation can still be used to model the expected movement of population across the tessellated model (see Deliverable D4.3 [5] for further details).

1.1.5 Risk Assessment

Cross-border harmonized risk assessment activities are currently being developed in order to integrate all available results in terms of data, approaches and tools into a consistent framework. Results will be shown in the upcoming deliverables.

3 AREA-FOCUSED RISK ACTIVITIES

Given the strong interdisciplinarity of the project and the inherent broad reach of risk management, many risk-related activities have been carried out during the first 18 months of the project in the different cross-border pilot areas. These activities are described in the following subsections in an aggregate, synthetic form, but in most cases a more detailed description is available in one of the past deliverables of the project. For each pilot areas the risk-related activities are grouped according to the specific risk assessment phase they refer to.

3.1 SOUTH TYROL

1.1.6 EXTREME EVENT ANALYSIS

The precipitation data used for the identification of most relevant events occurred in the period 1980-2020 were retrieved from the meteorological gridded dataset for Trentino-South Tyrol elaborated by EURAC (Crespi et al., 2021). It provides daily mean temperature and precipitation from 1980 onwards on a 250-m resolution grid covering the region and based on a high-quality and homogenized archive of weather station observations. According to the time coding adopted by the regional weather services, daily precipitation totals are defined as the cumulated precipitation between 8:00 UTC previous day to 8:00 UTC current day. In order to allow the comparison with Austrian gridded fields, precipitation data used in this deliverable were upscaled to 1-km resolution and the reference dates were aligned by shifting the time coding one day earlier. **See Deliverable D2.1** [4] **for further details**.

1.1.7 IMPACT DATA COLLECTION

Impact data collection strongly relied on support from local Civil Protection Department. **See Deliverables D3.2, D3.3** [7], [8] **for further details**.

ED30 hydrological event data base

The “Event Documentation of the 30th Division of the Autonomous Province of Bolzano (ED30)” (Macconi and Sperling, 2010) started in 1998. Over the years, the ED30 system, which allows organized and standardized surveys of hydrogeological events on watercourses (floods, debris

flows, landslides, falls and avalanches), has been continuously improved. After the notification of an event that has occurred, the investigation procedure starts with the dispatch of a documentalist and, if necessary, with the organization of a reconnaissance flight with the helicopter. The field work includes the collection of the main data of the process, the photo documentation and the elaboration of maps in the appropriate scale (at least 1:25,000). All these data are further digitized and archived in a database structured in modules. This dataset is a mere event database comprising over 1700 hydrological events in South Tyrol. Its 14 attributes contain information on the exact location (point geometry) and time on a daily basis of the event, details on the prevailing processes as well as on the affected water bodies; information about damages induced by these hazards are not included in this database. The ED30 hydrological event data base comprises the following hazard categories: “Overbank sedimentation”, “Landslide”, “Flood (inundation)” and “Urban flood”.

IFFI

The Geological Survey of Italy manages the national Italian landslide registry (“Inventario dei fenomeni franosi in Italia (IFFI)”). This inventory aims at identifying and mapping gravitational mass movements over the whole Italian territory, following standardized criteria.
This very comprehensive dataset includes over 11 000 landslide events characterized by 174 attributes for South Tyrol. These comprise information on the geographic location (district, municipality, point geometry), the type of hazard and its activity status, as well as - in about one fifth of entries - the exact date of the event. Other features deal with the damages induced by these events: personal injuries (deads, evacuated or injured), physical damages (e.g. to critical infrastructure) and costs. It has to be mentioned that not all information is available for every event.
Regarding hazard categories, IFFI differentiates between
“fall/topple”, “rotational/translational slide”, “complex”, “fast flow”, “deep-seated movement”, “slow flow”, “area with diffuse falls/topples”, “area with diffuse shallow slides”, “subsidence” and “area with diffuse subsidence”.

1.1.8 EXPOSURE MODELLING

The cross-border exposure model developed in TRANS-ALP **and described in deliverables D4.3 and D4.4 [5], [6]** has been further enhanced in South Tyrol by integrating a dynamic population model to account for changes between day-time, night-time and commuting time. This additional component, to be described in a paper and upcoming deliverable, is based on local data obtained from the Province of Bolzano and describing the relationship between home and work location for employees in the autonomous region. This will allow for a more precise characterization of exposure to multiple hazards. The approach will be possibly replicated to Austria and neighbouring Italian region by means of a statistical / machine learning approach.

3.2 EAST TYROL / AUSTRIA

1.1.9 EXTREME EVENT ANALYSIS

SPARTACUS

For the identification of relevant events in the time period from 1980 to 2020, weather data are taken from SPARTACUS, the "Spatiotemporal Re- analysis Dataset for Climate in Austria" (Hiebl and Frei, 2017). It provides high-quality, daily temperatures and precipitation-totals from 1961 onwards on a 1 km grid across Austria, Southern parts of Germany and South Tyrol. Precipitation totals are calculated from 7a.m. to 7 a.m..

SPARTACUS has been generated in an international collaboration from irregularly distributed weather stations and is operationally kept up-to-date at the Zentralanstalt für Meteorologie and Geodynamik in Vienna.

INCA

The goal of INCA is the optimal algorithmic combination of all currently available model and observation data in real time for the most detailed, high quality and reliable analysis and forecast of the current atmospheric state, especially in the Alpine region. After several years of development, the INCA analysis and nowcasting system is now in operational use. It provides hourly updated forecasts of temperature, humidity, wind, global radiation and quarter-hourly updated forecasts of cloud cover, precipitation and precipitation type for the whole of Austria on a 1-km grid. INCA analysis fields – which are used within TRANS-ALP – are available from 2004 onwards, depending on the parameter investigated.

See Deliverable D2.1 [4] **for further details**.

1.1.10 IMPACT DATA COLLECTION

In Austria, impact data collection relied on support from several local agencies. **See Deliverables D3.2, D3.3** [7], [8] **for further details**.

WLK

The Austrian Service for Torrent and Avalanche Control ("Wildbach und Lawinenverbauung" (WLV)), founded in 1884, is a subordinate agency of the Austrian Federal Ministry of Agriculture, Regions and Tourism (BMLRT). WLV traditionally deals with torrents and avalanches, which mainly occur within the alpine region. Amongst WLV's tasks are: declaration of danger zones potentially yielding settlement-prohibitions, civil protection management and providing advisory capacity towards climate-change adaption. These (and many more) responsibilities require diligently collected long-term records of hazard-processes that are compiled in the "Wildbach- und Lawinenkataster (WLK)" (WLV, 2017). It covers fluvial sediment transport processes, which are floods containing amounts of solids up to one fifth their volume; debris-flow-like processes – as before,

but with a fraction of solid material exceeding one fifth; mud flows, carrying solid contents exceeding 50%; flooding; and surface water. Landslides are distinguished into rotational slides, which are movements exhibiting a rotation about an axis parallel the slopes; translational slides, i.e. slides with negligible rotation; earth- and debris flows, where the material sliding down is subjected to strong deformation; shallow landslides; individual blocks with block sizes up to 1 m; large blocks with sizes exceeding one meter; as well as rock creeps (Enigl et al., 2019).

GEORIOS

Founded in 1849, the Geological Survey of Austria ("Geologische Bundesanstalt" (GBA)) is a subordinate agency of Austrian Federal Ministry for Education, Science and Research (BMBWF). Fields of activity encompass geological mapping, process-monitoring and issuing of maps featuring high-risk areas for planning purposes. Just as in case of WLV, the accomplishment of GBA's governmental obligations requires a highly dependable, comprehensive, and statistically robust data basis. Such sound, conscientiously collected, long-term records of damage-events are compiled in "Geologischen Risiken Österreich (GEORIOS)" database (Tilch et al., 2011). Therefore, various observation systems are employed. Amongst these are, for example, remote-sensing, field surveys, geographical photographs, systematic expert-inventories of indexed areas, reports from the population and the digitization of historical archives. To avoid inhomogeneities, which may result from different formats, quality criteria and degrees of information content, GBA devotes a substantial fraction of its resources to maintain an extensive quality assurance program, ensuring just that. GBA-records used in this study start in 1950 and cover the following gravitational processes: slides, flows, falls, general mass movements, mass movements in loose rock, and complex large-scale movements (Enigl et al., 2019).

Meteorological data

Weather data are taken from SPARTACUS, the "Spatiotemporal Reanalysis Dataset for Climate in Austria" (Hiebl and Frei, 2015; 2017). It provides high-quality, daily temperatures and precipitation-totals from 1961 onwards on a 1 km grid across Austria and South Tyrol. SPARTACUS has been generated in an international collaboration from irregularly distributed weather stations maintained by ZAMG, has already found application in several studies (Duethmann and Blöschl, 2018; Schroeer and Kirchengast, 2018) and is operationally kept up-to-date at ZAMG (Enigl et al., 2019).

1.1.11 Mapping of windthrow

The windthrow areas were determined and recorded by the Amt der Tiroler Landesregierung (state of Tyrol) using airborne laser scan surveys. A DSM was generated, which was compared with a DSM before the storm event. By subtracting the DSM after Vaia from the DSM before Vaia ("NDSM"), it was possible to identify those areas where significant changes in vegetation cover have occurred (windthrow).

1.1.12 Analysis of Cascading effects

The field site in Kals am Großglockner in East Tirol was established as an experimental field site to investigate and understand how the trees downed by the storm Vaia in 2018 affect the snowpack and, thus, the snow avalanche hazard. The investigation started with Step 2, where terrain roughness was identified as a potential key variable. The forest damage assessment (Step 1) was carried out by applying different methods. First an overview of the forest damage was obtained via high-resolution satellite and manned aircraft orthophotos in the region of East Tirol. Further investigation was done on the ground by manual inspection by a group of foresters and researchers (see Figure 14) and with UAS flights to retrieve a detailed overview of the forest damage at the experimental test site (Figure 15).

Figure 14: Visiting the study site for the first time (10 Oct 2021) (left); aerial view of the lower section of the site with Kals a.G. in the background, recorded with a DJI Mavic 2 Pro on the same day (right).

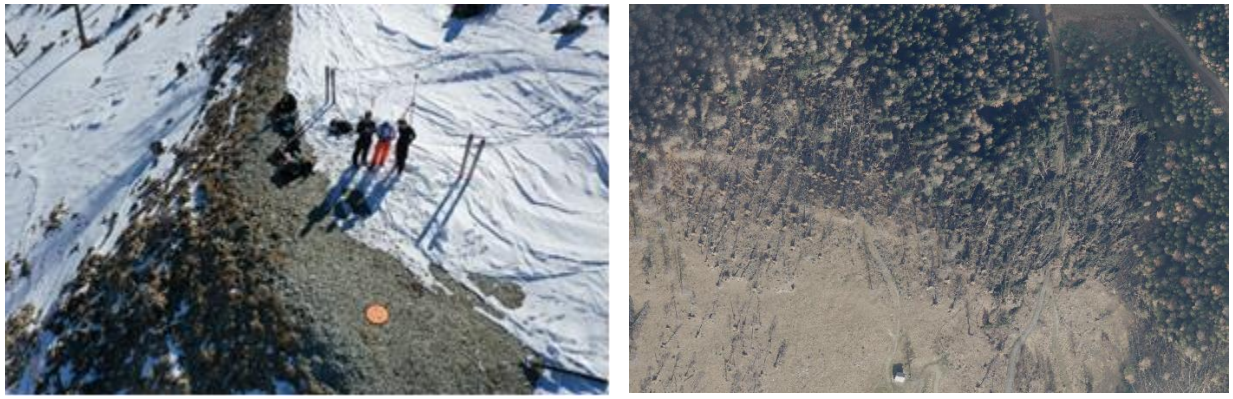

Figure 15: Aerial view of the fieldwork team positioned on a blown-off section of the forest road winding through the study site with the snow in the vicinity showing strong signs of wind influence (left); post-event orthophoto commissioned by the LFD documenting the extent of forest damage following the wind throw event at the study site in 2018 (right) (source: LFD, Land Tirol).

Current work is being done to determine the most suitable roughness algorithm for describing the directional surface roughness. The software needs to balance the robustness detail of the directional roughness index with the computer processing time for such a calculation, which is challenging because point cloud data can be computationally heavy. In addition, a plethora of measurements on the snowpack properties and layering was carried out in three measurement campaigns throughout the 2021 -2022 winter season.

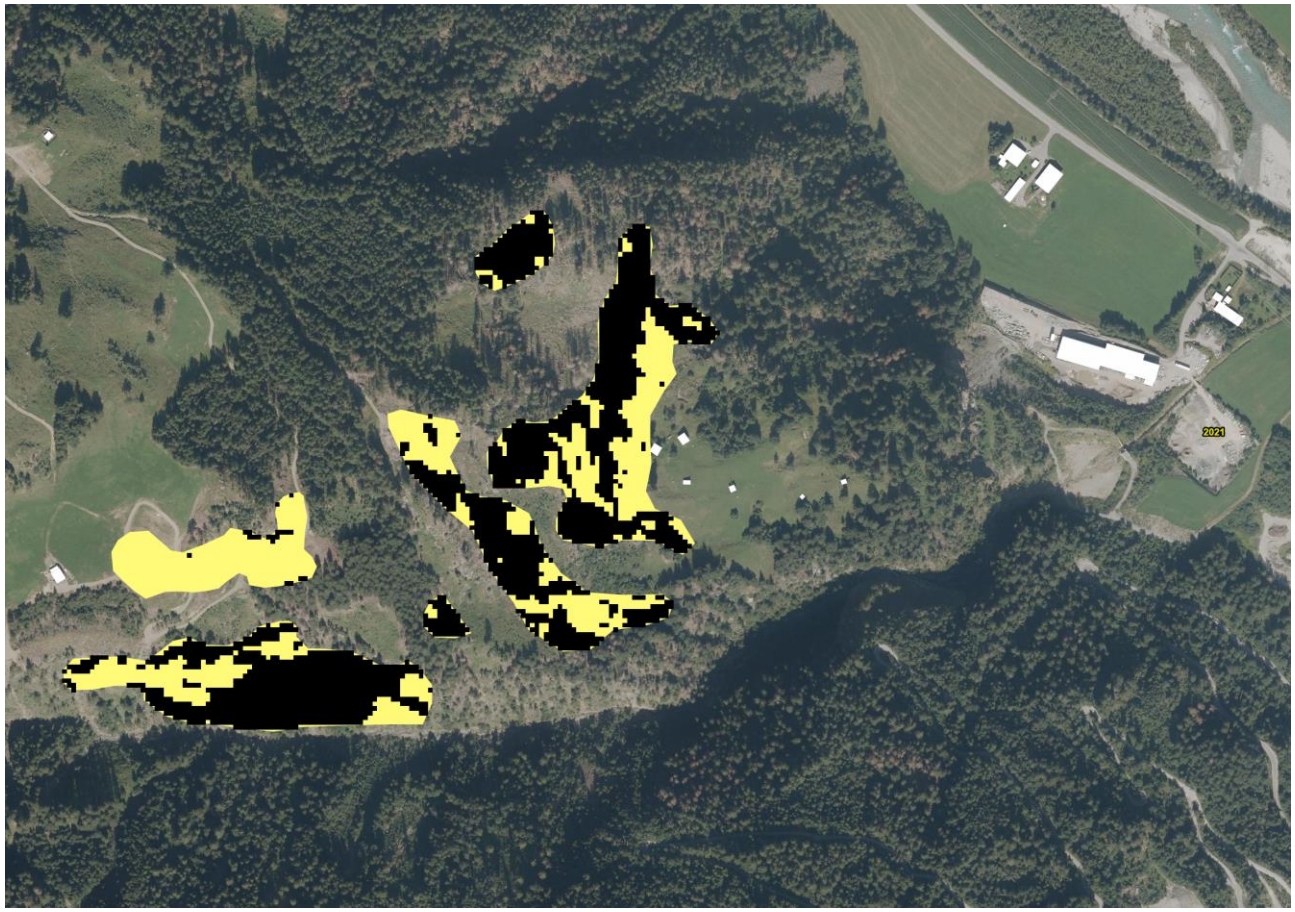

Figure 16: Example of cleared windthrow areas (yellow shapes) and terrain sections inside, which are at inclinations between 34° and 55° (black pixels). Those black pixels are PRAs and are included in the avalanche simulations with Flow-Py.

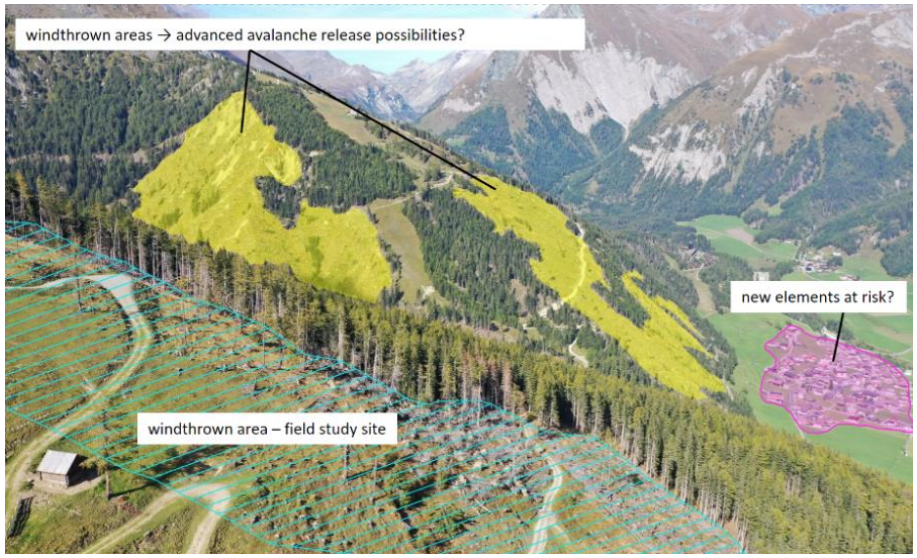

Figure 17: Windthrow in the area of the ski resort Kals, the hamlet of Großdorf at the bottom site and the BFW´s field study site in the front.

Figure 17 shows a landscape record from Kals taken while a drone flight in the frame of field studies in Kals am Großglockner. The yellow areas show windthrown forest sites which are already cleared an now potentially function as avalanche release areas. The village of Kals (hamlet Großdorf colored in Magenta) was suddenly after VAIA 2018 exposed to a number of natural hazards including avalanches, rockfall and landslides. In case of Kals it is to be mentioned, that a multifaceted set of mitigation measures was installed in a short time (release fences). Nevertheless, still many of newly exposed infrastructures are now situating in East Tyrol, where mitigation measures where not constructed up to now.

The Figure 18 shows an overview of the entire East Tyrol. The light blue to dark blue ranging pixels show the modelled avalanches and their paths starting in cleared Vaia windthrow areas respectively from the above described new avalanche release areas (Figure 16). As visible in the Figure, large areas nearly over the entire East Tyrol could potentially endanger infrastructures situated in main and side valleys of this district. Hotspot regions for new avalanche hazard scenarios are the center of East Tyrol including the Kalsertal, Hopfgarten in Defereggen and Huben in the middle of the Iseltal (see white box in Figure 18). **See Deliverable D3.3** [7] **for further details**.

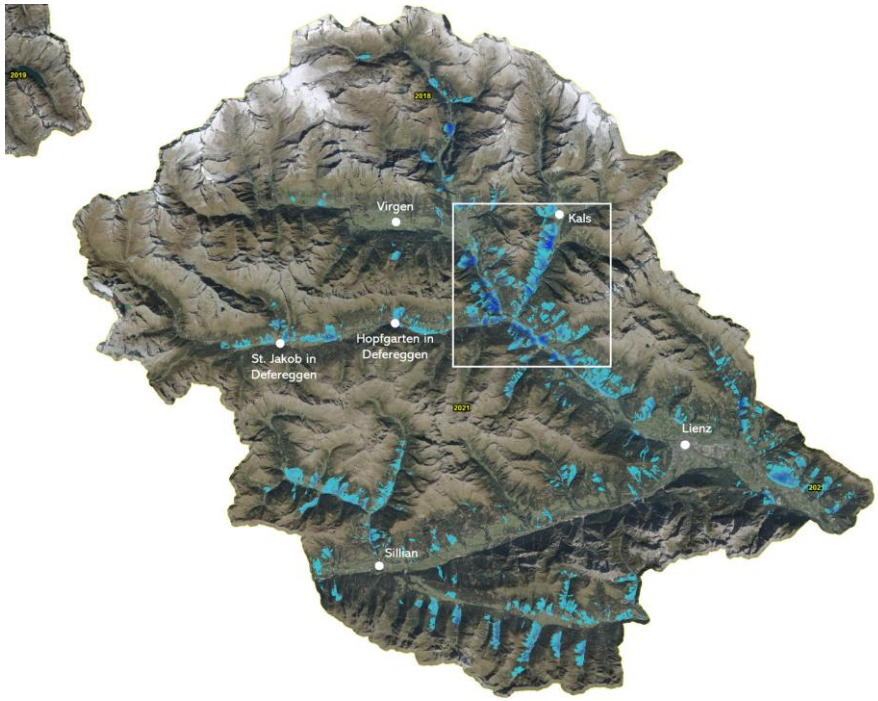

Figure 18: the entire area of East Tyrol (district Lienz) covered with new potential avalanche paths, potentially released in cleaned windthrow areas. Generated in the Flow-Py model. Most affected area highlighted in the white box.

1.1.13 INCREASE OF AVALANCHE RISK DUE TO WINDTHROW

The example depicted in Figure 19 shows several small villages in East Tyrol connected by a primary road (red line) and the current hazard zone plan elaborated from the Austrian Avalanche and Torrent Control. From this current hazard zone plan, the yellow zone (furthest reaching relevant avalanche pressures) is visualized. The yellow arrows indicate the general avalanche flow direction. Considering this hazard zone plan, the major road (red line) is affected by avalanches on a short section highlighted in the white rectangle. Under consideration of newly established release areas after the Vaia windstorm (black pixels), the potential avalanche runout distance partly increases up to about 150 meters. The consequence is a longer section of the road network potentially affected by the modelled avalanche (black rectangle) and therefore an intensified risk scenario.

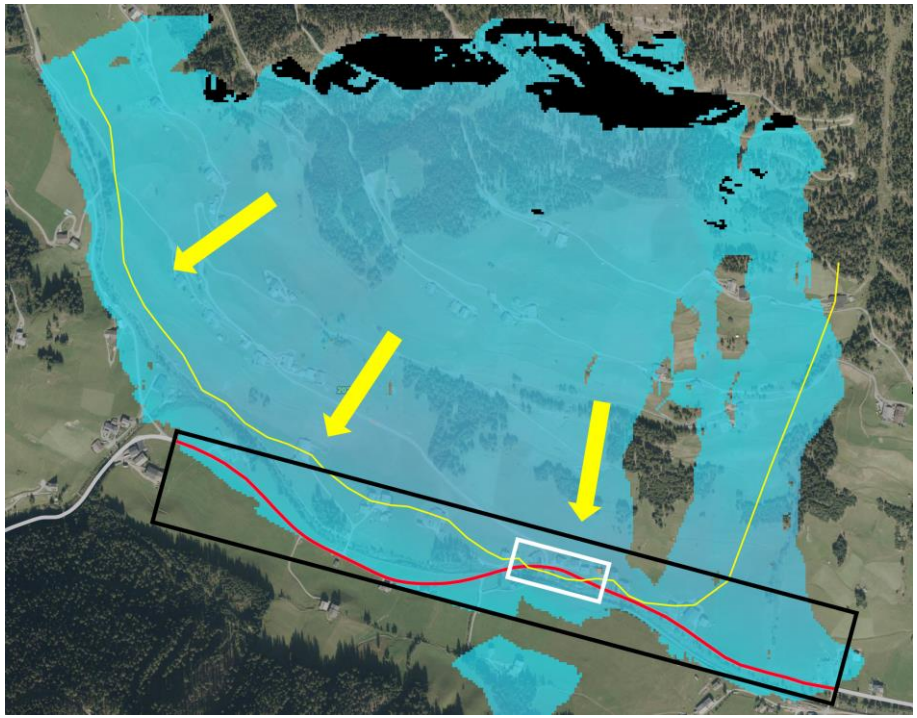

Figure 19 Change in exposure to avalanche resulting from numeric simulation of avalanches.

is depicted in Figure 20. Although this shows a so-called spatially relevant settlement area, i.e. area that needs to be protected (black dashed line), no yellow and red danger zones for avalanches have been designated in the center of the hamlet because there was no corresponding exposure up to now. Storm Vaia has resulted in such a large gap in the protection forest that, with appropriate simulations, a new risk scenario can now be assumed and the adaptation of the hazard zone plan could be initiated. **See Deliverable D3.3** [7] **for further details**.

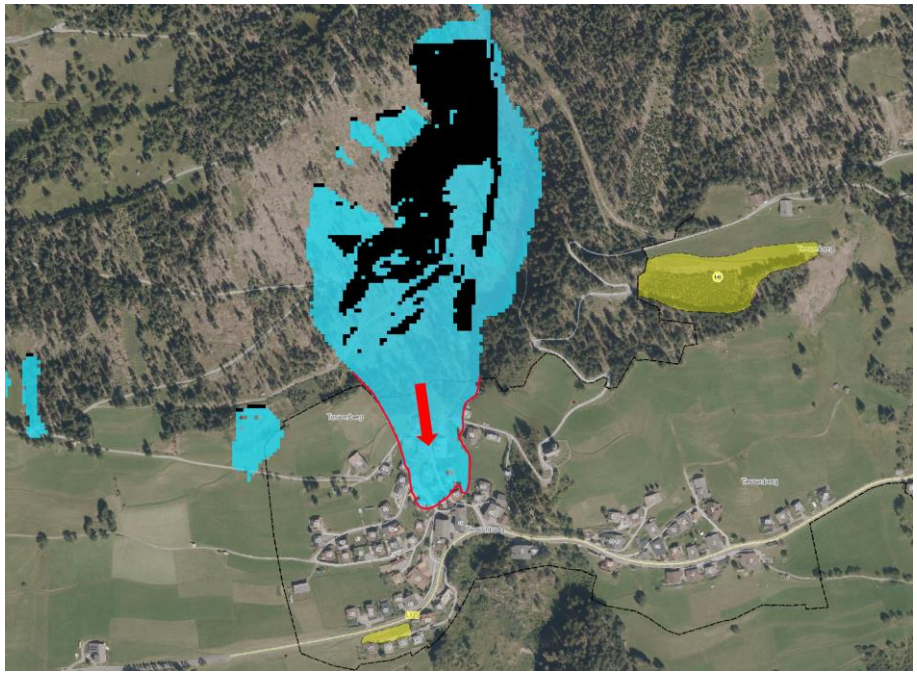

Figure 20: current danger zone plan from the avalanche and torrent control (yellow shapes). The blue signature highlights new potential avalanche paths generated in the cleaned windthrow area above the hamlet. Source hazard zone plan: Land Tirol / Tiris

3.3 AGORDINO VALLEY

1.1.14 EXTREME EVENT ANALYSIS

Regarding Veneto, in the TRANS-ALP project ARPAV decided to develop a multihazard approach at a local scale, in a small alpine basin. For the identification of relevant events in the time period from 1984 to 2020, weather data are taken from the automatic meteorological stations managed by ARPAV, a first approach was based on analyzing the meteorological events that had recorded significant ground effects in this basin. Nevertheless, in order to validate the methodology proposed here, and to try to harmonize the data with those of Trentino Alto

Adige and Austria, raster maps of daily cumulative precipitation were created using data from the Veneto weather stations network for the dates indicated in Table 1. Data from more than 180 rain gauges were interpolated for each date.
At a later stage, in order to test the methodology of the 99th percentile in the study area, ARPAV evaluated the statistic of cumulative rainfall precipitation and the identified extreme events. The definition of the 99th percentile of precipitation was based on the historical series of every single rain gauge in the study area, ground effects were checked whenever the weather events was considered extreme by at least 3 rain gauges out of 13. **See Deliverable D2.1** [4] **for further details**.

1.1.15 Mapping of windthrow

Immediately after the event, an initial estimate of the damage was produced to manage the emergency phase quickly, but it was only after several months that remote sensing data became available to allow more precise monitoring of the forest damages. The databases used in this monitoring activity refer to Sentinel-2 satellite images (both pre- and post-event acquisitions were used), with the integration, where available, of post-event orthophotos. The following vegetation indices were compiled from satellite images: Normalized Difference Vegetation Index (NDVI), Red Edge Normalized Vegetation Index, Normalized Difference Water Index, and Green Normalized Difference Vegetation Index. For each index, the difference (post-event index)-(pre-event index) was calculated. Only more than one year after the storm event, a lidar flight acquiring data to compute a Digital Elevation Model (DEM) and DSM of all affected areas has been made available.
In the days immediately following the event, the technicians of the Arabba Avalanche Centre of ARPAV, manually mapped all the areas of downed forest that insisted on vulnerable elements. This methodology, although unorthodox, has nevertheless made it possible to speed up the creation of specific civil protection plans to mitigate the avalanche risk to the population. Such plans were already operational in use during the winter season following the storm. In the same days, the landslide mapping office of the Veneto Region conducted a series of inspections and collected specific data on damages, including to forest, which could affect the slope stability. **See Deliverables D3.2, D3.3** [7], [8] **for further details**.

1.1.16 Modelling of Avalanche susceptibility

The advantage of a morphological-based approach to identify the runout of potential avalanches is that it allows simultaneous analysis over large areas to identify potential hazard areas in a short time (see Figure 21).

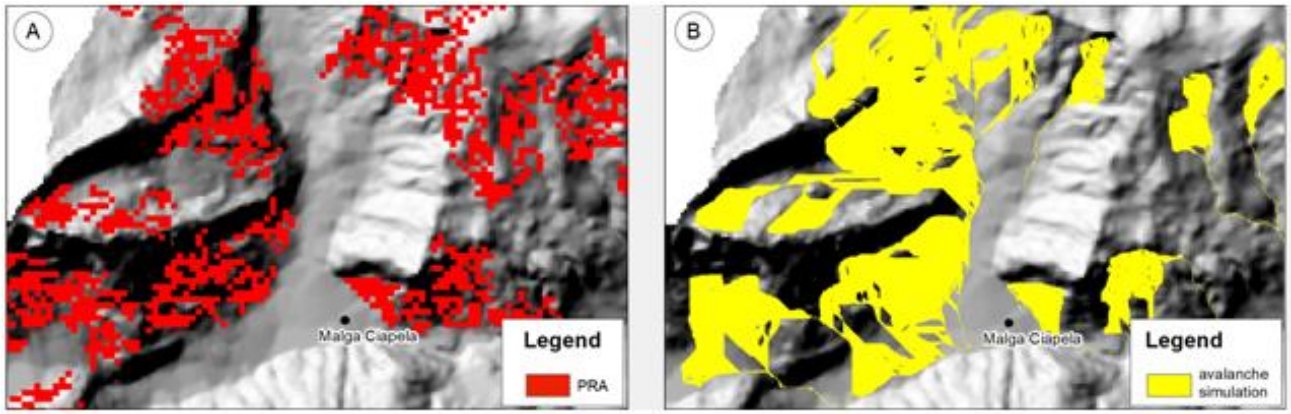

Figure 21: Example of how the tool developed by the Arabba Avalanche Centre (ARPAV) works: Once the PRA have been identified (A); from these, the runout of all potential avalanches in the study area are simulated simultaneously (B)

The tool developed by the Arabba Avalanche Centre is capable of reporting the avalanche susceptibility for the entire study area, which refers to the proneness of an area to avalanche occurrence. The main difference with the PRA map is that the latter is a binary map that identifies the avalanche release areas and differentiates them from the rest of the area. Instead, the susceptibility map, based on morphological characteristics, exposure and land use, proposes a scaling of the probability of avalanche release. In contrast to the tool that identifies PRAs, the susceptibility map samples the entire study area by splitting it according to different degrees of proneness to the release of the avalanche phenomenon. Years of field research have revealed that occurrence of avalanches is mainly affected by terrain, weather, vegetation cover and snowfall. In the tool developed, the terrain factors mainly included elevation, slope, aspect, plan curvature, profile curvature, terrain ruggedness index (TRI), topographic position index (TPI), Distance to Stream (DTS), topographic wetness index (TWI), Distance to Road and solar radiation, which were derived from analysis of the DEM. For the land-use map, the official map of the Veneto Region was used, from which the portion of vegetation destroyed by the Vaia storm was removed, considering the downed trees as bare ground. Each individual map was subdivided by its various parameters and, thanks to a statistical cross-reference with the avalanches recorded in the study area, each individual parameter was indexed by importance. The final result is a map that identifies areas which are subject to avalanches and measured from very low to very high susceptibility (Figure 22), and this aspect is fundamental for proper future land-use planning. **See Deliverable D3.3** [7] **for further details**.

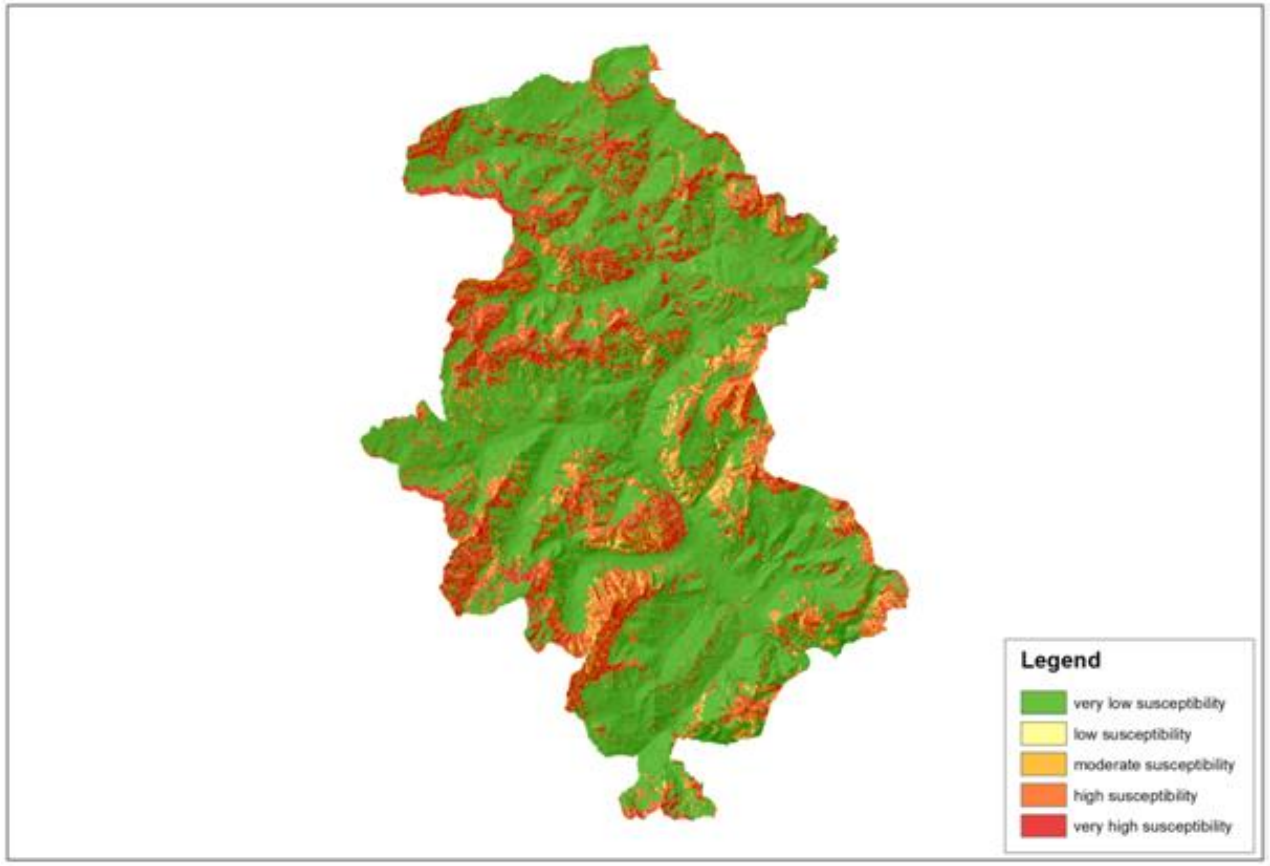

Figure 22: Avalanche susceptibility map of the Cordevole Valley

Here too an attempt was made to analyze the difference in model processing before and after the effects of the Vaia storm. Figure 23 clearly illustrates how the effects of the storm on vegetation affects all degrees of avalanche proneness.

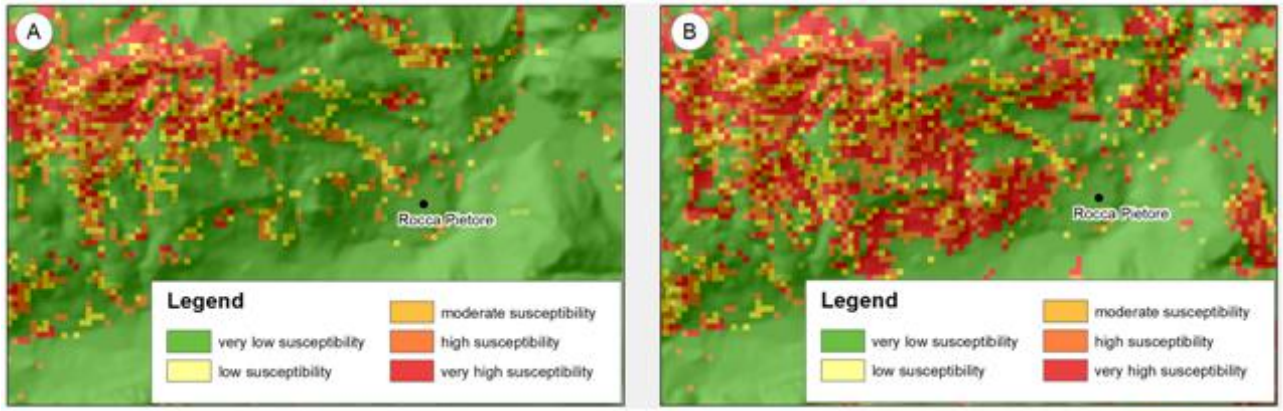

Figure 23: Susceptibility map evaluated by the tool developed by the Avalanche Centre of ARABBA (ARPAV). A) with the pre-storm Vaia forest condition; B) with the post- storm Vaia forest condition.

The final result is a raster map in which each element at risk has been indexed (Figure 24). Such indexing allows the identification of a priority for action in risk mitigation. **See Deliverable D3.3** [7] **for further details**.

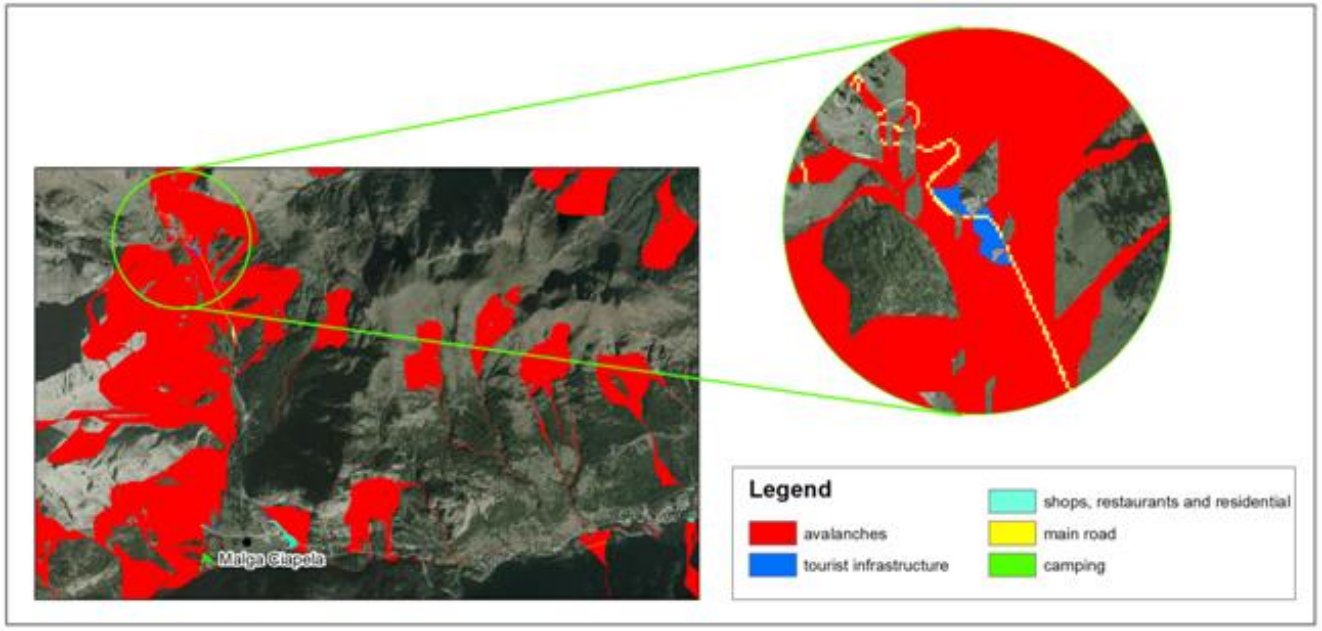

Figure 24: The map of the elements at risk as calculated by the application developed by the Arabba Avalanche Centre overlaid on the avalanche map

Once the areas characterized by a higher degree of vulnerability have been identified, a series of dynamic modelling was conducted to indicate along the avalanche path the maximum flow heights, impact pressures and the perimeter of the avalanche itself (Figure 25). It also considered the parameters relating to the characteristics of the snowpack and the friction that can develop at the specific site for different return periods. The numerical simulations have been realized using the software RAMMS, developed by the WSL Institute for Snow and Avalanche Research SLF (Christen et al., 2010).

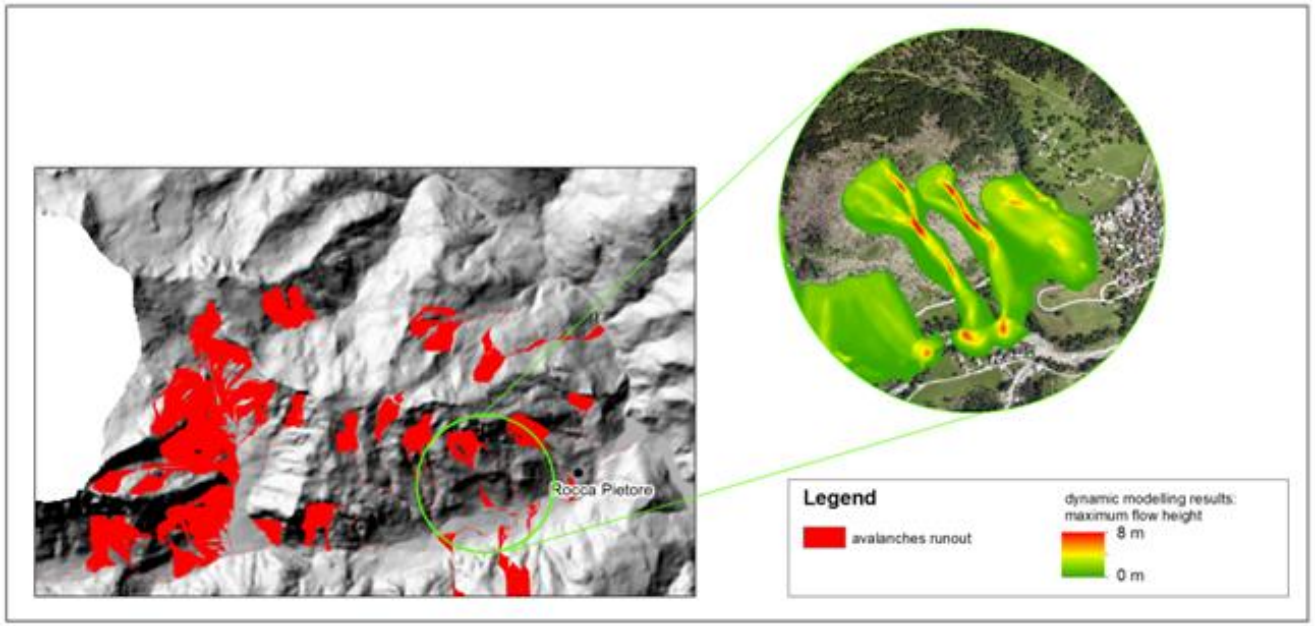

Figure 25: The box shows the dynamic modelling of avalanches that may affect the vulnerable elements identified using the tool developed by the Arabba Avalanche Centre. The example shows the maximum flow height.

The results of this final modelling were used for the implementation of special civil protection plans and will be applied in the future, when the countermeasures work will be completed, for the reclassification of avalanche hazards in accordance with the current national legislation.

The final result is a detailed plan for more than 60 sites in the Cordevole Valley, that includes daily monitoring of HN3gg in special snow observation sites performed by civil protection volunteers, and when the above thresholds are reached, it is clearly indicated on the map which houses have to be evacuated and which roads have to be closed to traffic (Figure 26). **See Deliverable D3.3** [7] **for further details**.

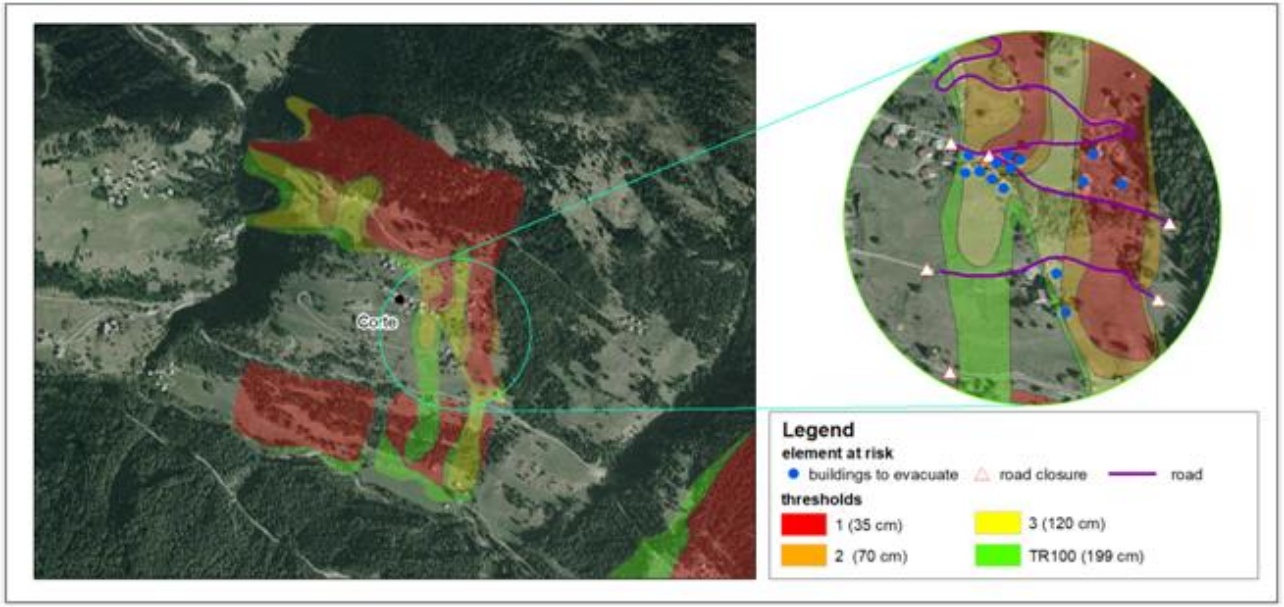

Figure 26: The risk classification in Lasta Sief site as a function of ground snow thresholds recorded. In the box is outlined which houses must be evacuated depending on the DH3gg threshold reached and where the road should be closed to traffic.

1.1.17 HARMONIZED POST-EVENT MULTI-HAZARD SURVEY FORMS

A series of post-event multi-hazard survey sheets are proposed. They have been structured through a general sheet in which the data relating to the place of the survey, the type of event and impact (landslide, avalanche, forest destroyed and beetle spread), the surveyors and the other people present at the inspection, the survey of the damages and the specification of the interference with a watercourse are noted. **See Deliverable D3.3** [7] **for further details**.

4 Conclusions

This document preliminarily describes the risk-related activities carried out in the three main cross-border pilot areas of the TRANS-ALP project. A two-tier approach is being followed, where overarching, cross-border activities (described in section C) are based on – and integrated by – local activities taking place in the individual pilot areas. This approach allows to obtain harmonized, cross-border products within a consistent risk assessment framework, but at the same time accounting for the specificities of the different pilot areas (in terms of data availability, capacities and available resources, specific needs and constraints, etc.). This approach will be further pursued in the last phase of the project with the aim of fostering a smooth but steady integration and harmonization of local practices (often of excellent value) with cross-border guidelines, indications and tools which are paramount to achieve transnational harmonization and to further improve regional-scale management of risk due to extreme hydrometeorological events.

5 References

[1] "TRANS-ALP Deliverable D2.2 - Hazard Datasets," EURAC. [Online]. Available: https://maps.eurac.edu/documents/1124
[2] "TRANS-ALP Deliverable D2.3 - Hazard set, under climate change," EURAC, Deliverable. [Online]. Available: https://maps.eurac.edu/documents/1125
[3] "TRANS-ALP Deliverable D2.4 - Storm hazard and climate change," EURAC, Deliverable. [Online]. Available: https://maps.eurac.edu/documents/1126
[4] "TRANS-ALP Deliverable D2.1 - Storm hazard and climate change," EURAC, Deliverable. [Online]. Available: https://maps.eurac.edu/documents/1123
[5] "TRANS-ALP Deliverable D4.3 - Exposure and vulnerability modelling," EURAC, Deliverable. [Online]. Available: https://maps.eurac.edu/documents/1131
[6] "TRANS-ALP Deliverable D4.4 - Exposure dataset," EURAC, Deliverable. [Online]. Available: https://maps.eurac.edu/documents/1133
[7] "TRANS-ALP Deliverable D3.3 - Analysis of cascading effects," EURAC, Deliverable. [Online]. Available: https://maps.eurac.edu/documents/1134

[8] “TRANS-ALP Deliverable D3.2 - Guidelines for harmonizing impact data collection.” [Online]. Available: https://maps.eurac.edu/documents/1128